

2020-03-01

Stochastic evolutionary-based optimization for rapid diagnosis and energy-saving in pilot- and full-scale Carrousel oxidation ditches

Li, L

<http://hdl.handle.net/10026.1/17666>

10.3808/jei.201700377

Journal of Environmental Informatics

International Society for Environmental Information Science (ISEIS)

All content in PEARL is protected by copyright law. Author manuscripts are made available in accordance with publisher policies. Please cite only the published version using the details provided on the item record or document. In the absence of an open licence (e.g. Creative Commons), permissions for further reuse of content should be sought from the publisher or author.

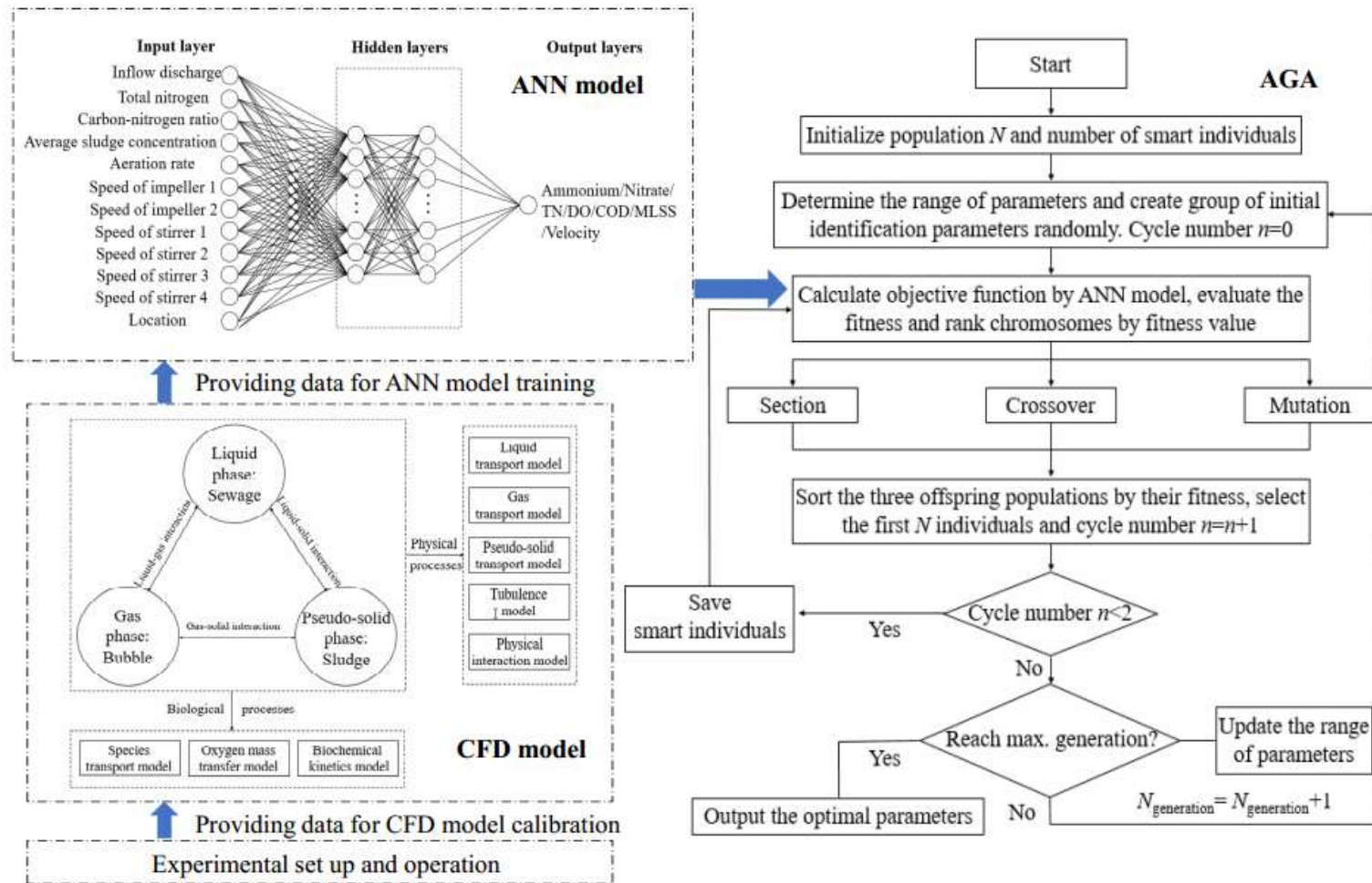


Fig. 1 Framework of hybrid model of conditions in the oxidation ditch, comprising a three-dimensional (3D) three-phase computational fluid dynamics (CFD) model, multi-site artificial neural network (ANN) model and accelerating genetic algorithm (AGA) model.

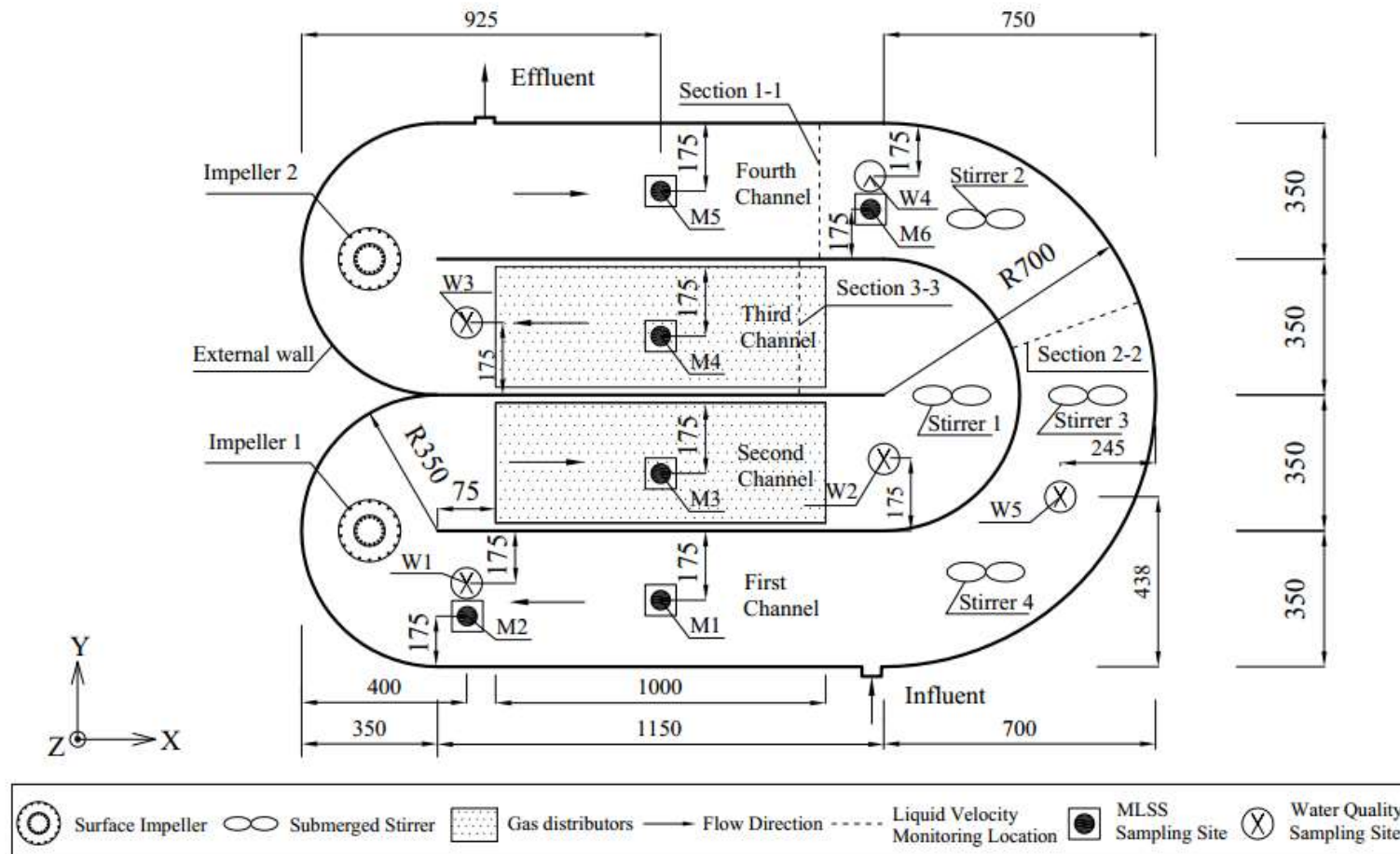


Fig. 2 Schematic of pilot-scale oxidation ditch and monitoring sites (Unit: mm).

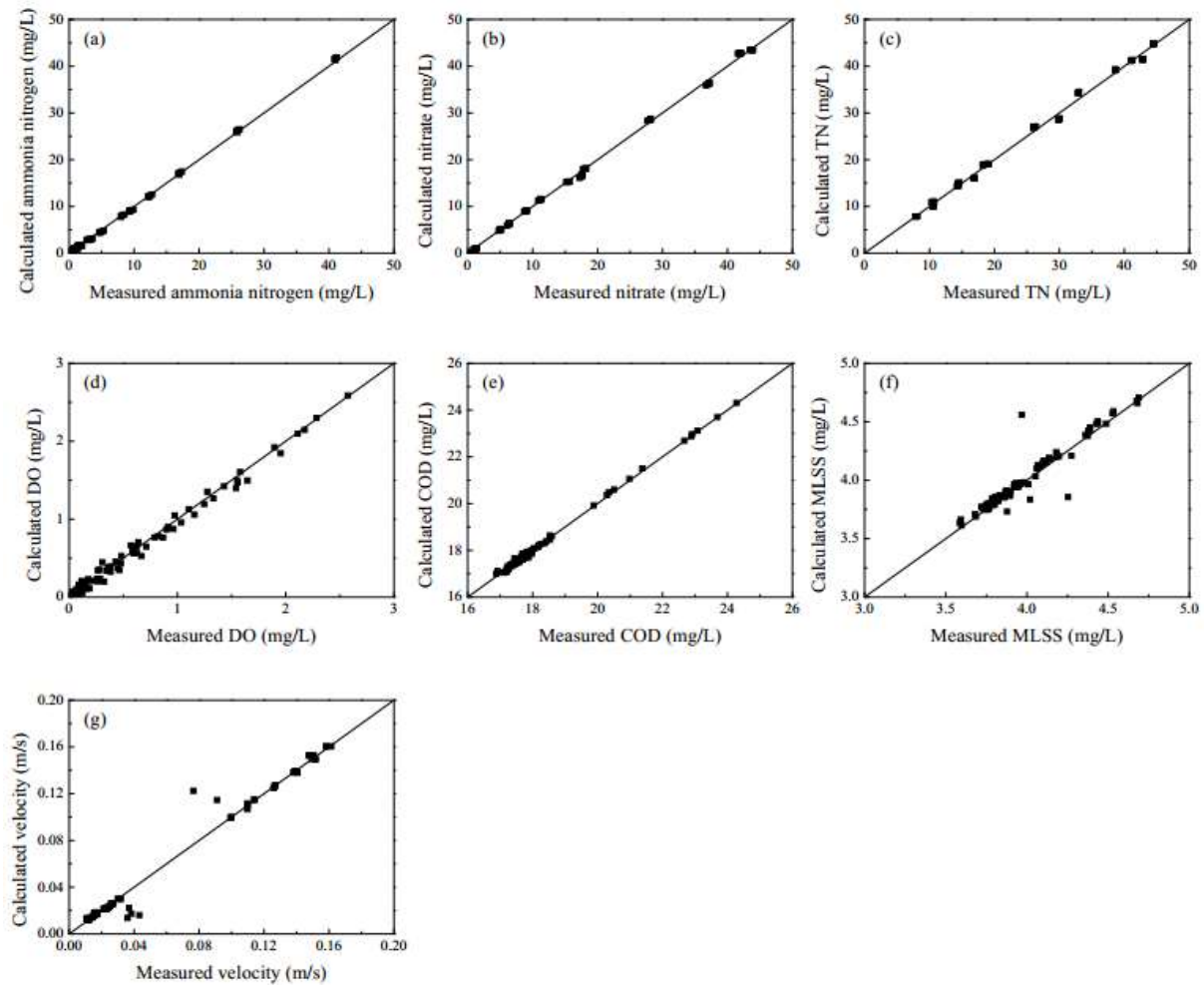


Fig. 3 Comparisons between calculated and measured values of: (a) ammonia nitrogen concentration; (b) nitrate concentration; (c) TN concentration; (d) DO concentration; (e) COD concentration; (f) MLSS concentration; and (g) liquid velocity in a pilot-scale OD.

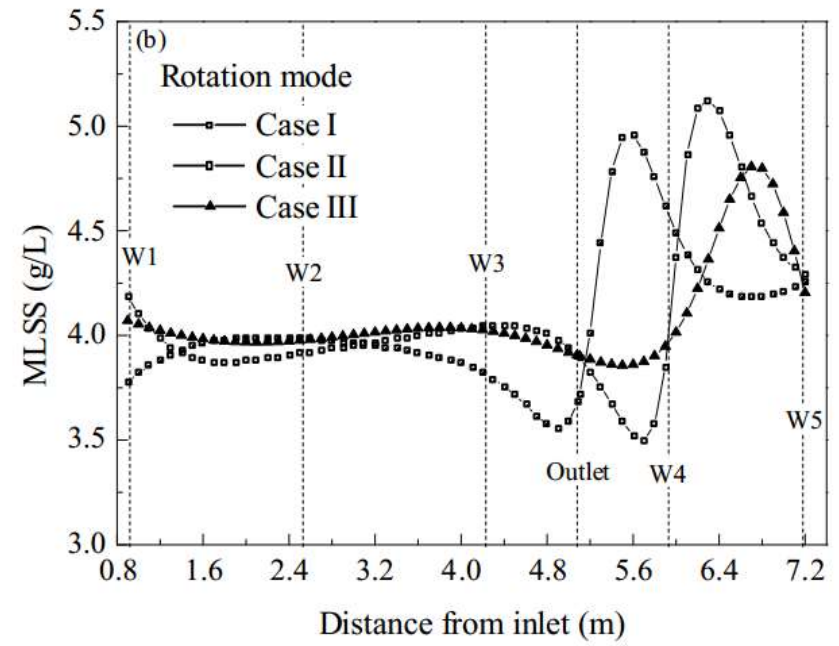
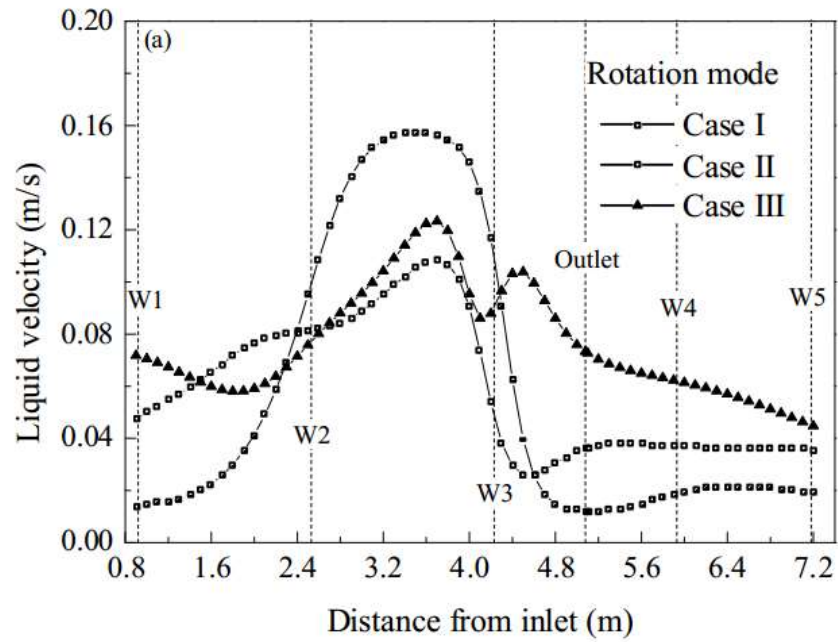


Fig. 4 Stream-wise profiles of (a) predicted liquid velocity and (b) concentration of MLSS at elevation 0.1 m above the bottom of the pilot-scale oxidation ditch, for an aeration rate of $1.4 \text{ m}^3/\text{h}$.

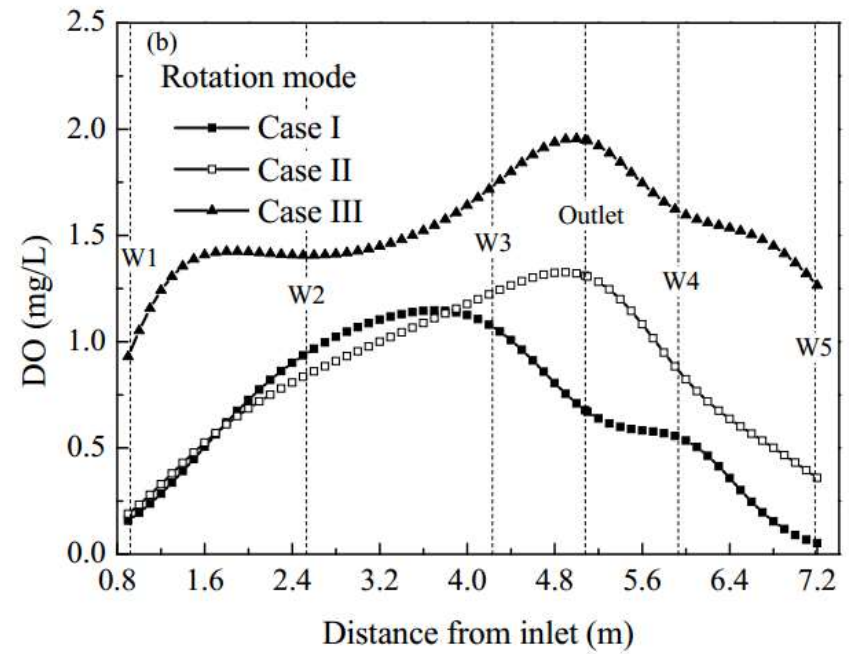
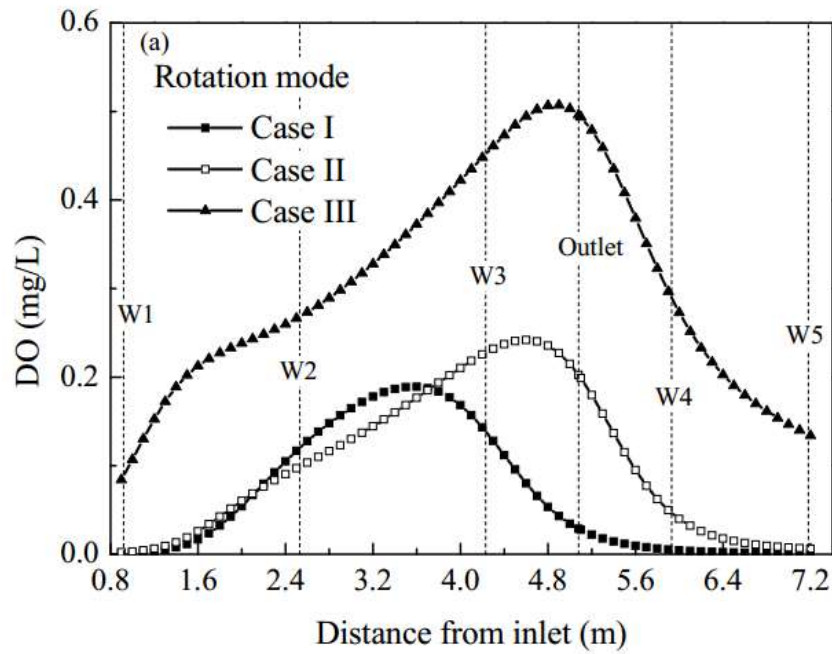


Fig. 5 Stream-wise profiles of dissolved oxygen at elevation 0.1 m above the bottom of the pilot-scale oxidation ditch, for aeration rates of (a) $1.4 \text{ m}^3/\text{h}$ and (b) $3.0 \text{ m}^3/\text{h}$.

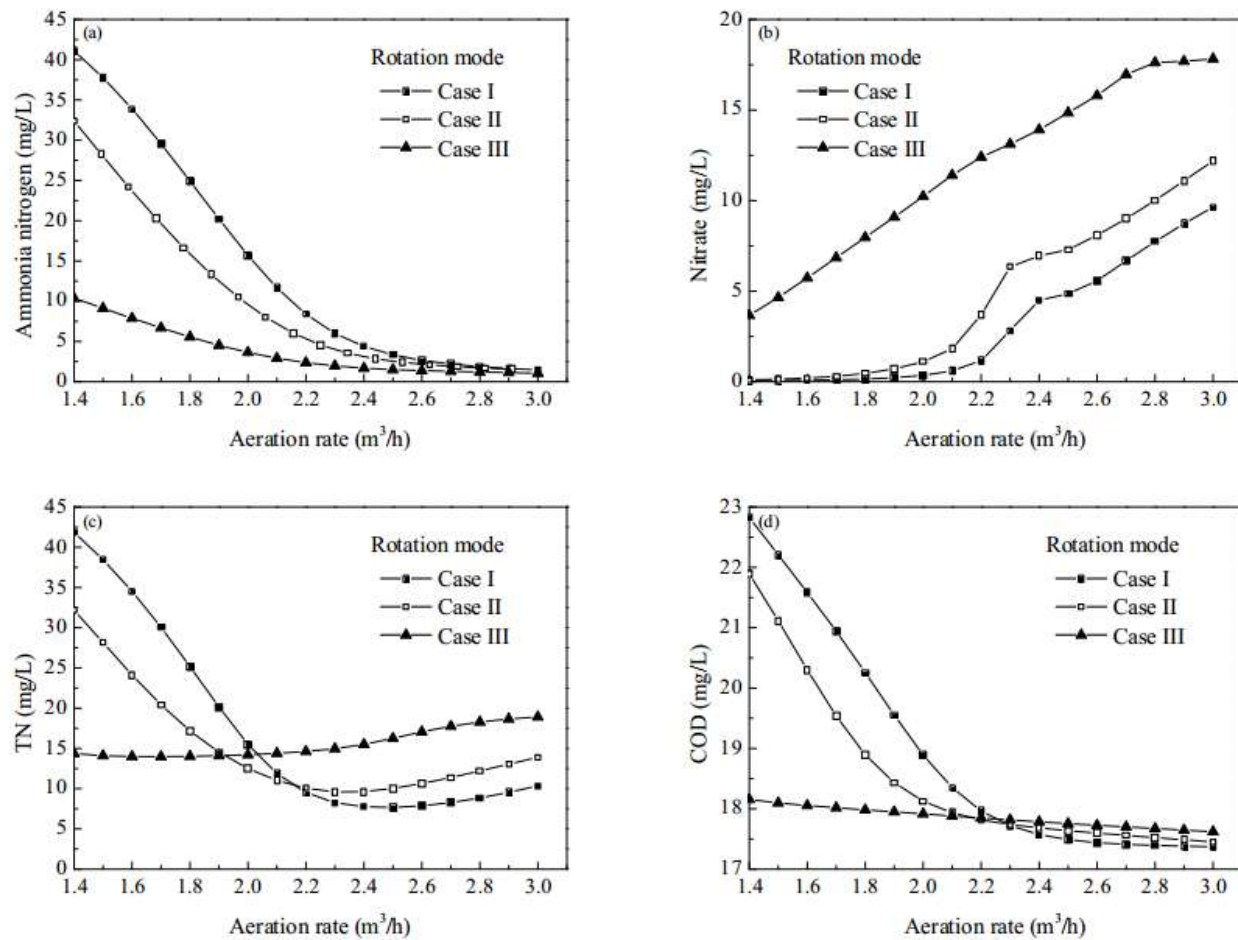


Fig. 6 Predicted effluent concentrations of (a) ammonia nitrogen, (b) nitrate, (c) TN, and (d) COD as functions of aeration rate, at an elevation 0.25 m above the bottom of the pilot-scale OD under three different operation modes.

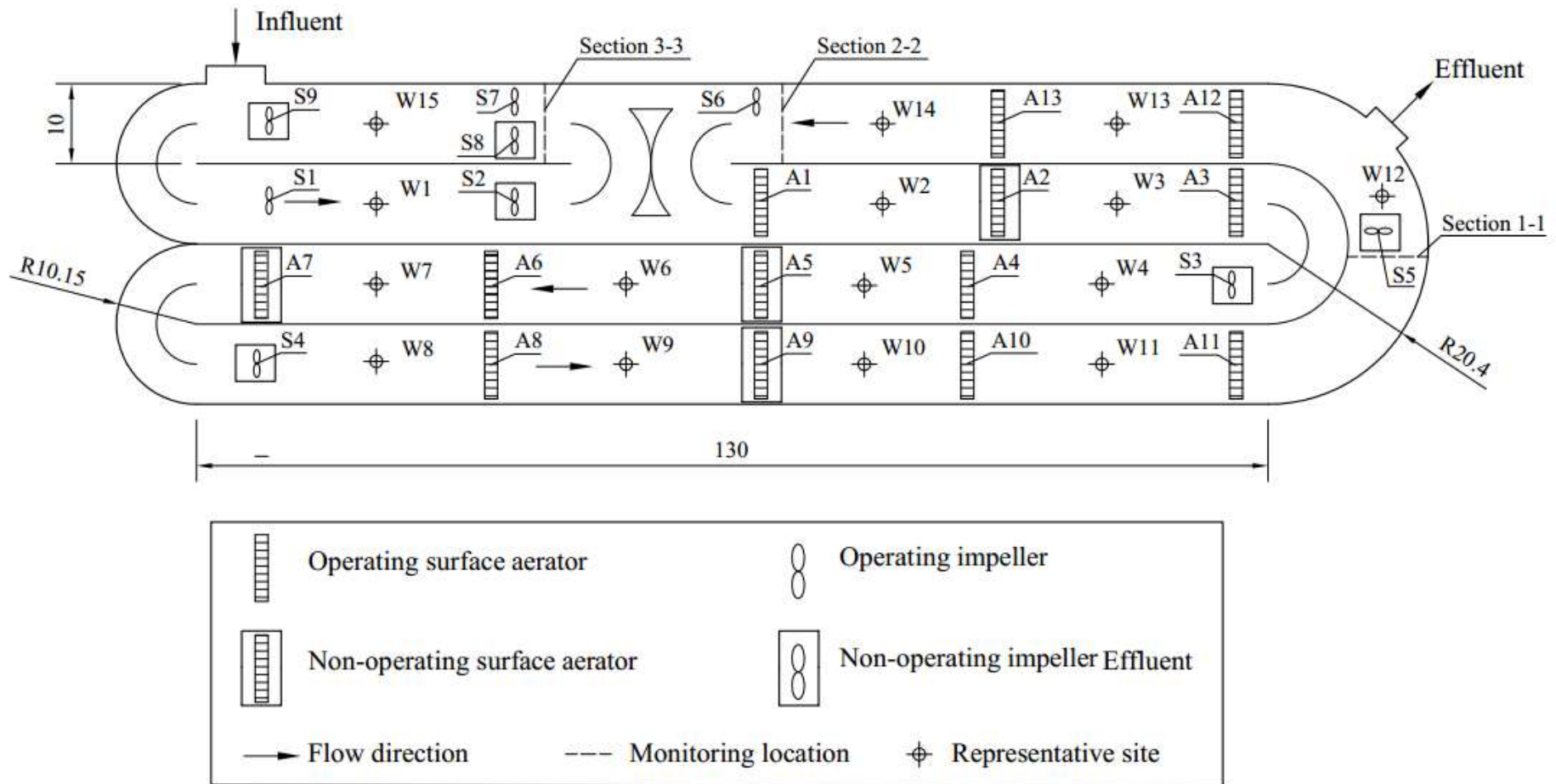


Fig. 7 Full-scale oxidation ditch and monitoring sites, Ping Dingshan, Henan Province, China (Unit: m).

Table 1 Rotational modes of impellers and stirrers.

Moving part	Case I		Case II		Case III		Case IV	
	Speed (rpm)	Direction	Speed (rpm)	Direction	Speed (rpm)	Direction	Speed (rpm)	Direction
Impeller 1	40	+ ¹	80	+	180	+	40	+
Impeller 2	40	+	80	+	180	+	40	+
Stirrer 1	40	- ²	90	-	120	-	70	-
Stirrer 2	40	+	90	+	120	+	70	+
Stirrer 3	40	+	90	+	120	+	70	+
Stirrer 4	50	+	70	+	115	+	50	+

¹ + clockwise rotation.

² – anticlockwise rotation.

Table 2 Experimental conditions for testing the ANN model in the pilot-scale oxidation ditch.

Inflow discharge (L/h)	TN (mg/L)	Carbon-nitrogen ratio	MLSS (g/L)	Aeration rate (m ³ /h)	Speeds of impellers and stirrers
100	50	3	3.9	1.4	Case IV
100	50	3	3.9	1.8	Case IV
100	50	3	3.9	2.2	Case IV
100	50	3	3.9	2.6	Case IV
100	50	3	3.9	3	Case IV
100	50	5	3.9	1.4	Case IV
100	50	5	3.9	1.8	Case IV
100	50	5	3.9	2.2	Case IV
100	50	5	3.9	2.6	Case IV
100	50	5	3.9	3	Case IV
100	50	7	3.9	1.4	Case IV
100	50	7	3.9	1.8	Case IV
100	50	7	3.9	2.2	Case IV
100	50	7	3.9	2.6	Case IV
100	50	7	3.9	3	Case IV

Table 3 Optimum structures and test results of the ANN model in the pilot-scale oxidation ditch.

Variable	Structure	MSE	OF	R ²
Ammonia nitrogen	12-11-10-1	7.34×10^{-2}	0.33%	0.9996
Nitrate	12-8-13-1	2.21×10^{-1}	0.32%	0.9990
TN	12-14-4-1	5.69×10^{-1}	0.33%	0.9963
DO	12-7-14-1	3.34×10^{-3}	1.13%	0.9922
COD	12-12-9-1	4.87×10^{-3}	0.04%	0.9982
MLSS	12-14-13-1	7.38×10^{-3}	0.23%	0.9031
Liquid velocity	12-11-8-1	5.26×10^{-5}	1.36%	0.9822

Table 4 Optimized operating condition in the pilot-scale OD.

Operation condition							Effluent quality					\bar{v}^9	E^{10}
x^1	a^2_1	a_2	b^3_1	b_2	b_3	b_4	NH^4	NO^5	TN^6	DO^7	COD^8	\bar{v}^9	E^{10}
1.60	46.35	43.02	47.06	55.73	78.67	88.76	4.36	0.14	4.50	0.01	25.0336	0.07	216.90

x^1 : aeration rate, m^3/h ; a^2 : rotating speed of impeller, rpm; b^3 : rotating speed of stirrer, rpm; NH^4 : concentration of ammonia nitrogen, mg/L; NO^5 : concentration of nitrate, mg/L; TN^6 : concentration of total nitrogen, mg/L; DO^7 : concentration of dissolved oxygen, mg/L; COD^8 : concentration of COD, mg/L; \bar{v}^9 : averaged liquid velocity, m/s; E^{10} : energy consumption, W.

Table 5 Optimum structures and test results of the ANN model in the full-scale oxidation ditch, Ping Dingshan, Henan Province, China.

Variable	Structure	MSE	RSD	R ²	BLE
Ammonia nitrogen	23-15-13-1	0.2701	0.17%	0.9864	y=0.9973x+0.0571
Nitrate	23-14-4-1	0.1570	0.59%	0.9523	y=0.9602x+0.085
TN	23-14-9-1	0.3416	0.14%	0.9704	y=0.9952x+0.0709
COD	23-12-2-1	2.4733	0.21%	0.9886	y=0.9786x+0.5775
Liquid velocity	23-7-8-1	0.0004	0.60%	0.9216	y=0.9421x+0.0078

R²: Correlation coefficient

BLE: Best linear fitting equation

Table 6 Optimized operating condition in full-scale OD, Ping Dingshan, Henan Province, China.

Number	Surface aeration													Submerged impeller									Effluent quality				\bar{v}^7	E ⁸
	A1	A2	A3	A4	A5	A6	A7	A8	A9	A10	A11	A12	A13	S1	S2	S3	S4	S5	S6	S7	S8	S9	NH ³	NO ⁴	TN ⁵	COD ⁶		
1	0 ¹	1 ²	0	1	0	1	0	1	0	1	0	0	1	0	0	1	0	1	1	0	0	1	4.76	9.08	13.84	30.19	0.16	238.76
2	0	1	0	1	0	1	0	1	0	1	0	0	1	1	0	1	0	1	0	0	0	1	4.12	3.39	7.51	30.04	0.16	238.76
3	0	1	0	1	0	1	0	1	0	1	0	1	0	0	0	1	0	1	0	1	0	1	4.43	2.46	6.89	28.65	0.16	238.76
4	1	0	0	1	0	1	0	1	0	1	0	0	1	1	0	1	0	1	0	0	0	1	4.89	4.64	9.53	29.96	0.16	238.76
5	1	0	0	1	0	1	0	1	0	1	0	1	0	0	0	1	0	1	0	1	0	1	2.48	4.01	6.49	29.76	0.16	238.76

0¹: Non-operation; 1²: Operation; NH³: concentration of ammonia nitrogen, mg/L; NO³: concentration of nitrate, mg/L; TN⁵: concentration of total nitrogen, mg/L; COD⁶: concentration of COD, mg/L; \bar{v}^7 : averaged liquid velocity, m/s; E⁸: energy consumption, kW.